*Tellus (2006), 58B, 620–627*
*Printed in Singapore. All rights reserved*


**TELLUS**

# Biogeophysical effects of $CO_2$ fertilization on global climate

*By* G. BALA[1]*, K. CALDEIRA[2], A. MIRIN[1], M. WICKETT[1], C. DELIRE[3] and T. J. PHILLIPS[1], [1]*Energy and Environment Directorate, Lawrence Livermore National Laboratory Livermore, CA 94550, USA;* [2]*Department of Global Ecology, Carnegie Institution, Stanford, CA 94305, USA;* [3]*ISE-M, Université Montpellier II, 34095 Montpellier Cedex 5, France*

(Manuscript received 24 October 2005; in final form 27 June 2006)

ABSTRACT

$CO_2$ fertilization affects plant growth, which modifies surface physical properties, altering the surface albedo, and fluxes of sensible and latent heat. We investigate how such $CO_2$-fertilization effects on vegetation and surface properties would affect the climate system. Using a global three-dimensional climate-carbon model that simulates vegetation dynamics, we compare two multicentury simulations: a 'Control' simulation with no emissions and a 'Physiol-noGHG' simulation where physiological changes occur as a result of prescribed $CO_2$ emissions, but where $CO_2$-induced greenhouse warming is not included. In our simulations, $CO_2$ fertilization produces warming; we obtain an annual- and global-mean warming of about 0.65 K (and land-only warming of 1.4 K) after 430 yr. This century-scale warming is mostly due to a decreased surface albedo associated with the expansion of the Northern Hemisphere boreal forests. On decadal timescales, the $CO_2$ uptake by afforestation should produce a cooling effect that exceeds this albedo-based warming; but if the forests remain in place, the $CO_2$-enhanced-greenhouse effect would diminish as the ocean equilibrates with the atmosphere, whereas the albedo effect would persist. Thus, on century timescales, there is the prospect for net warming from $CO_2$ fertilization of the land biosphere. Further study is needed to confirm and better quantify our results.

## 1. Introduction

When the atmospheric $CO_2$ concentrations increase, the land biosphere can take up more $CO_2$ per unit of water loss. This makes more carbon available for building woody material, favouring forested ecosystems over grasslands. In northern latitudes, these effects would tend to select boreal forests over tundra, since the former absorb more solar radiation and warm the surface (Bonan et al., 1992). This warming would also tend to make conditions less harsh, thus favouring the spread of boreal forests (Foley et al., 1994; Grace et al., 2002). Alterations in evapotranspiration due to $CO_2$-fertilization-induced changes in stomatal conductance and the amount of leaf area could also impact the climate. Here, we investigate the climate effects of such $CO_2$-induced changes in vegetation physiology, structure and distribution.

When water and nutrients are available, photosynthesis by land plants is expected to increase with atmospheric $CO_2$ content via the so-called $CO_2$-fertilization effect (Owensby et al., 1999), leading to increased carbon uptake. Higher $CO_2$ concentrations promote water-use efficiency of plants, leading to stimulated plant growth (Polley et al., 1993). However, increased global temperatures also result in increased heterotrophic soil respiration rates (Lloyd and Taylor, 1994), diminishing or even reversing the net $CO_2$ flux from the atmosphere to the land biosphere (Cox et al., 2000; Friedlingstein et al., 2001; Thompson et al., 2004; Zeng et al., 2004; Govindasamy et al., 2005; Mathews et al., 2005).

Thompson et al. (2004) showed that $CO_2$ fertilization could strongly damp the global warming but nutrient limitations could weaken this effect. They performed a 'Fertilization' simulation in which the land biosphere used the model-predicted atmospheric $CO_2$ concentration, and a 'Saturation' simulation in which the effects of $CO_2$ fertilization were assumed to be saturated at year 2000 atmospheric $CO_2$ levels. The Saturation simulation represented the possibility that nutrients or other factors could limit the $CO_2$-fertilization effect. The land biosphere was a very strong sink of carbon in the Fertilization simulation through the year 2100, but it became a source of carbon to the atmosphere in the Saturation case.

However, $CO_2$ fertilization can have climate consequences in three other ways. First, it has the potential to modify the surface properties by enhancing plant growth, changing the vegetation distribution and altering the surface albedo (Levis et al., 1999,

*Corresponding author.
e-mail: bala@llnl.gov
DOI: 10.1111/j.1600-0889.2006.00210.x

2000). Second, $CO_2$ fertilization promotes water use efficiency by inducing stomatal closure (Polley et al., 1993; Owensby et al., 1999), producing warming via a reduction of evapotranspiration (Henderson-Sellers et al., 1995; Sellers et al., 1996), and possibly also an increase in runoff (Gedney et al., 2005). Finally, $CO_2$ fertilization may enhance leaf area and increase evapotranspiration (Betts et al., 1997), which would have a cooling effect. We refer to the collective impacts of these vegetation changes on the physical climate as the 'biogeophysical' effects of $CO_2$ fertilization. In contrast, we refer to the potential amelioration of the greenhouse radiative impact of $CO_2$ resulting from its sequestration by vegetation as the 'biogeochemical' effects of $CO_2$ fertilization.

How large are the biogeophysical effects of $CO_2$ fertilization? In equilibrium experiments (run over a few decades) using a mixed layer ocean model coupled to atmospheric and dynamic vegetation models, Levis et al. (1999) showed that vegetation changes due to a doubling of $CO_2$ could produce a warming of about 1.5 °C in summer and spring in the high latitudes. The warming was mainly brought about by reduction in surface albedo; however, there was no global mean warming in their decadal simulations (Levis et al., 2000). In a simulation that did not include the radiative effects of increasing $CO_2$ concentrations, Cox et al. (2000) obtained a slight warming over land by the year 2100 due to $CO_2$-induced changes in stomatal conductance and vegetation distribution. In their coupled climate-carbon model simulation, Notaro et al. (2005) obtained a global mean warming of about 0.1 K during the historical period (pre-industrial to present-day) due to the physiological effects of increasing atmospheric $CO_2$. The warming signals in Levis et al. (2000), Cox et al. (2000) and Notaro et al. (2005) were small because the simulations were run for only a few decades or a century. However, dynamic changes in vegetation distribution could take many centuries.

Using a coupled climate-carbon cycle model that simulates vegetation dynamics (Bala et al., 2005; Govindasamy et al., 2005), we compare two *multicentury* simulations in this study: a 'Control' simulation with no emissions, and a 'Physiol-noGHG' simulation with prescribed emissions. The Physiol-noGHG simulation allows $CO_2$ fertilization and other physiological changes, but has no direct $CO_2$-induced greenhouse climate change. Our simulations indicate that $CO_2$ fertilization could produce a biogeophysical climatic effect of warming over a timescale of a few centuries that would offset at least part of the biogeochemical effect of cooling. We find that this warming is mostly associated with an albedo decrease resulting from the expansion of the Northern Hemisphere boreal forests.

## 2. Model

To investigate the $CO_2$ fertilization impacts of climate change due to anthropogenic emissions, we use INCCA (INtegrated Climate and CArbon), a coupled climate and carbon cycle model (Thompson et al., 2004; Bala et al., 2005; Govindasamy et al., 2005) developed at Lawrence Livermore National Laboratory (LLNL). The physical ocean-atmosphere model is the NCAR/DOE PCTM model (Meehl et al., 2004), which is a version of the NCAR CCM 3.2 model (Kiehl et al., 1996) coupled to the Los Alamos National Laboratory's POP ocean model (Maltrud et al., 1998). The climate model is coupled to a terrestrial biosphere model, the Integrated Biosphere Simulator version 2 or IBIS2 (Foley et al., 1996; Kucharik et al., 2000) and to a prognostic ocean biogeochemistry model based on the diagnostic Ocean Carbon-cycle Model Intercomparison Project (OCMIP) Biotic protocols (Najjar and Orr, 1999). The horizontal resolution of the land and atmosphere models is approximately 2.8° in latitude and 2.8° in longitude, while the ocean model has a horizontal resolution of (2/3)°. The atmosphere and ocean models have 18 and 40 vertical levels, respectively. Flux adjustments are not applied to the physical climate model.

## 3. Experiments

We perform two model simulations starting from year-1870 pre-industrial initial conditions created by more than 200 yr of spin up: a Control case with no $CO_2$ emissions for the period 1870–2300, and a Physiol-noGHG case in which emission rates are prescribed out to year 2300, as discussed in Bala et al. (2005). In the Control case, climate drift for the period 1900–2300 is a –0.62 K ($\sim -0.15$ per century) change in mean surface temperature, and a 3.8 ppmv increase in atmospheric $CO_2$ concentration. The drift in sea ice area and volume for this 400 yr period are $+15.3\%$ and $+40\%$, respectively.

In the Physiol-noGHG case, the land and ocean carbon cycle models use the predicted atmospheric $CO_2$ content associated with the prescribed emissions, but the radiation calculation uses the pre-industrial concentrations of $CO_2$ and other greenhouse gases: there is no change in greenhouse gas radiative forcing for the period 1870–2300, and hence there is no $CO_2$-enhanced greenhouse climate change. This is the (perhaps misnamed) 'constant-climate' simulation as discussed in several coupled climate-carbon cycle modelling studies (e.g. Cox et al., 2000; Friedlingstein et al., 2001; Govindasamy et al., 2005). The results from the corresponding fully interactive climate-carbon experiment are discussed in Bala et al. (2005).

As described in Bala et al. (2005), for our Physiol-noGHG case, $CO_2$ emissions are specified at historical levels for the period 1870–2000 (Marland et al., 2002) and at SRES A2 levels for the period 2000–2100 (IPCC, 2001). For the years 2100–2300, emission rates follow a logistic function for the burning of the remaining conventional (coal, oil and natural gas) fossil-fuel resources (assuming 5270 gigatons of carbon (Gt C) in 1750; Metz et al., 2001). Non-$CO_2$ greenhouse gas concentrations are specified at historical levels for 1870–2000 and at SRES A2 levels for 2000–2100 (IPCC, 2001) and are fixed at 2100 levels thereafter. Land use emissions are taken from Houghton (2003)

for the historical period, and from the SRES A2 scenario for the years 2000–2100, and are set to zero thereafter. There is no change in aerosol forcing. The cumulative emission for the entire period 1870–2300 is 5404 Gt C. Increasing from the present day values of 8 Gt C per year, the emission rate peaks at about 30 PgC per year in the 22nd century around year 2120, and then it declines sharply in the 23rd century to almost zero by year 2300 (see Bala et al., 2005).

## 4. Results

Here, we focus our discussion on differences between the experiment (Physiol-noGHG) and Control simulations. Compared to the Control, the global- and annual-mean temperature in the Physiol-noGHG simulation begins to rise after year 2050 (Fig. 1a). This global-mean temperature increase coincides with the sharp rise in atmospheric $CO_2$ concentrations after the year 2050 (Fig. 1b). The warming is as high as 1K in the 22nd century; thus, $CO_2$ fertilization has the potential to change the global climate on centennial timescales. The global- and annual-mean warming in the last decade of our simulation (2291–2300) is 0.65 K (1.4 K over land) which will be considered as the INCCA model's estimate of biogeophysical impact of $CO_2$ fertilization in the rest of our discussion. The global mean temperature change 0f 0.65 K is only a little larger than the residual drift in the Control, but it is opposite in sign. Hence, there is no prima facie reason to assume that the drift in the control affects our basic conclusions.

In the Physiol-noGHG case, the atmospheric $CO_2$ concentration increases to1166 ppmv from its pre-industrial value of 289 ppmv (Fig. 1). When this coupled climate and carbon cycle model also included the simulation of the radiative effects of greenhouse gases, it predicted 1423 ppmv and an 8 K warming for the same emissions scenario (Bala et al., 2005). This result suggests that the radiatively driven $CO_2$-induced greenhouse warming (i.e. the climate-carbon cycle feedback) in this model contributes 257 ppmv to the atmosphere by 2300 through reduced land and ocean carbon uptake. The $CO_2$ concentration is decreasing (Fig. 1) near the end of the simulation (year 2300) due to the continued uptake of about ∼2 Gt C per year by both land and oceans (Fig. 2) when the emissions rates are almost zero (see Bala et al., 2005). Fig. 2 suggests that the response timescale for uptake by the land to increasing atmospheric $CO_2$ is much shorter (decades) than that by the oceans (centuries).

The global- and annual-mean change evinced by different climate variables (Physiol-noGHG case minus control in the

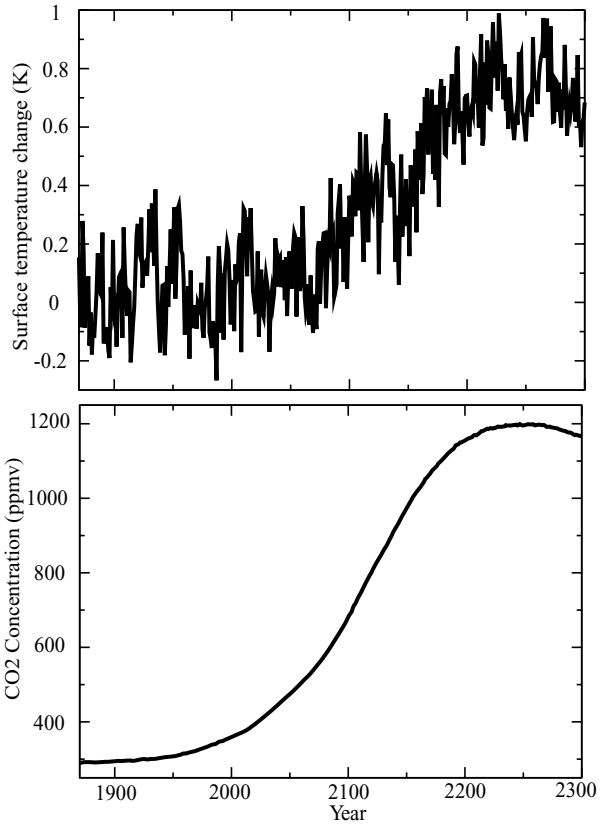


*Fig. 1.* Evolution of drift-corrected global- and annual-mean surface temperature (upper panel) and atmospheric $CO_2$ concentration (lower panel) in the Physiol-noGHG simulation. Mean surface temperature warming in the Physiol-noGHG case in the last decade (years 2291–2300) is about 0.658 K relative to Control, and the atmospheric $CO_2$ concentration is 1166 ppmv at year 2300.

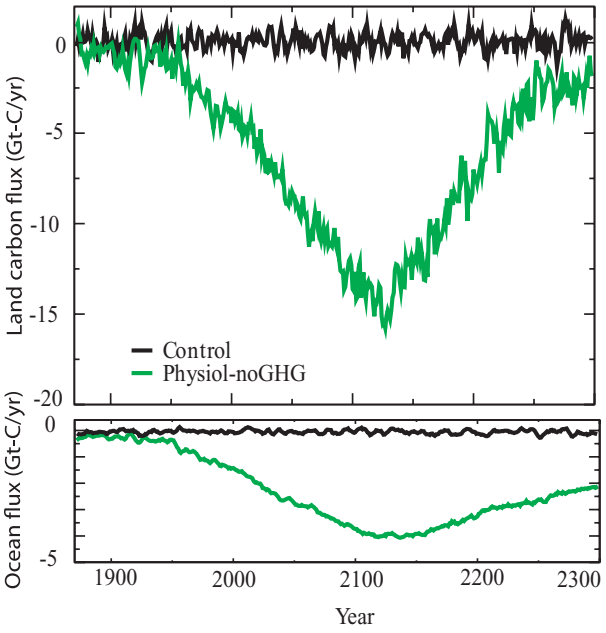


*Fig. 2.* Evolution of global- and annual-mean carbon fluxes between atmosphere and land (upper panel), and between atmosphere and ocean (lower panel) in the control and Physiol-noGHG simulations. Negative fluxes indicate uptakes of carbon by both land and oceans.

*Table 1.* Changes in global- and annual-means of climate variables in the Physiol-noGHG case (decade of 2291–2300 minus 1891–1900). The changes are corrected for the drift in the Control simulation

| Experiment | Surface temp. (K) | Precip. (%) | Sea ice extent (%) | Sea ice volume (%) | Net short wave flux at TOA ($Wm^{-2}$) | Net flux at TOA ($Wm^{-2}$) |
|---|---|---|---|---|---|---|
| Physiol-noGHG | 0.65 | 0.4 | −5.3 | −36.8 | 0.88 | 0.01 |

*Table 2.* Fraction of land area occupied by dominant vegetation types at the end of simulations in the Control and Physiol-noGHG cases (dominant vegetation during 2271–2300). In the Physiol-noGHG case, the forested and tundra fractions have increased, and those of grasslands and deserts have decreased

| Vegetation type | Control | Physiol-no GHG |
|---|---|---|
| Tropical forests | 22.1 | 26.3 |
| Temperate forests | 19.2 | 24.1 |
| Boreal forests | 6.4 | 10.4 |
| Savannah, grasslands and shrub lands | 12.4 | 7.0 |
| Tundra | 6.2 | 8.3 |
| Desert | 16.7 | 13.4 |
| Polar desert | 17.0 | 10.5 |

decade of 2291–2300) is shown in Table 1. For example, while the changes in global mean precipitation are negligible (less than 1%), the magnitude of change in ice volume is about 37%. The change in the net short wave absorption at the top of the atmosphere (TOA) is 0.88 $Wm^{-2}$. Assuming a radiative forcing of 3.4 $Wm^{-2}$ for a doubling of $CO_2$ and an equilibrium climate sensitivity of 2.1 K for this model (IPCC, 2001), this implies an equilibrium warming of about 0.55 K, which is in close agreement with the simulated transient warming of 0.65 K.

The vegetation distributions in the two experiments are listed in Table 2. IBIS2 simulates only the natural potential vegetation so that land-use changes are not included. There is an increase in the tropical, temperate and boreal forests due to $CO_2$ fertilization (Fig. 3). The total forested land fraction increases by 13%

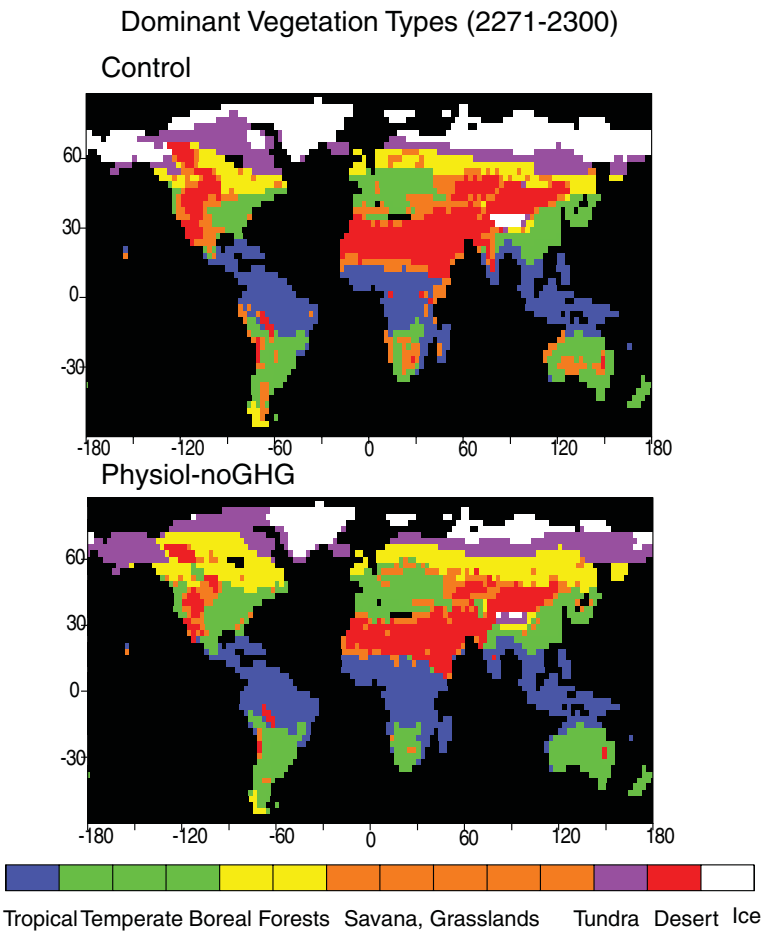


*Fig. 3.* Dominant vegetation distributions in Control (top panel) and Physiol-noGHG (bottom panel) cases in the last 30 yr of the simulations (2271–2300). Antarctica is not shown. There is an expansion of boreal forests into tundra regions in the Physiol-noGHG case, and the tundra vegetation moves into the land ice area of the control. The expansion of temperate forests also can be seen in Australia, South Africa and North and South America.

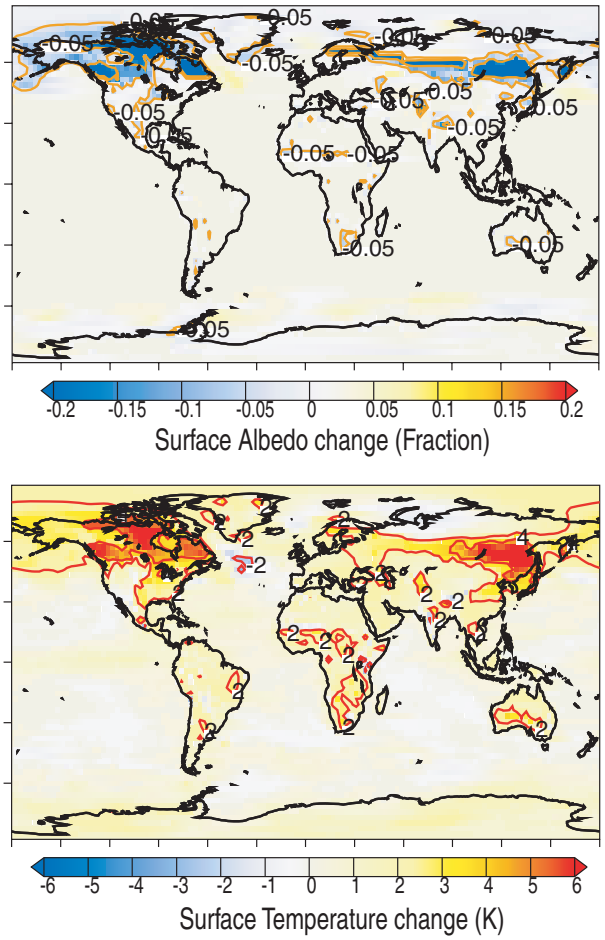


*Fig. 4.* Difference in surface albedo (top panel) and surface temperature (bottom panel) between the Physiol-noGHG and Control cases. The differences are computed over the decade 2291–2300. The expansion of forests at the expense of grasslands and savannah due to $CO_2$ fertilization leads to a decrease in the surface albedo and an increase in surface temperature over Northern high-latitude land areas.

of land area, with tropical, temperate and boreal forests expanding by about 4%, 5% and 4%, respectively (Table 2). During the same period, deserts, polar deserts, grasslands and savannah decline by a similar fraction. There is a northward expansion of boreal forests at the expense of tundra (Fig. 3), and tundra also moves northward into the land ice area. Grasslands, savannah and deserts are replaced by temperate forests in Australia, South Africa and North and South America. Tropical forests in Africa expand slightly to the north at the expense of savannah and grasslands. The $CO_2$-induced physiological changes in vegetation presumably help to counter effects of desertification that may occur as a result of climate change (Table 2). Because these changes to natural vegetation take many centuries to unfold, only models (such as the one used in this study) that include vegetation dynamics, and that can be run for multiple centuries, can adequately simulate the vegetation distribution changes.

However, our study also has some inherent limitations. We do not take into account the constraint that land use imposes on the development of natural ecosystems. In our Physiol-noGHG simulation, we only account for the global carbon emissions due to land use by taking Houghton's (2003) estimate for the historical period, the SRES A2 scenario for the period 2000–2100, and zero thereafter (Bala et al., 2005). Because the IBIS model allows only natural vegetation to grow, we do not simulate the effects of agricultural crops. Thus, forests would not actually be able to grow as simulated here because a large part of the land surface would be under some form of cultivation (Ramankutty et al., 2002). This would limit carbon uptake by the land biosphere because most cultivated ecosystems do not accumulate biomass, and under current management practices, very small amounts of litter enter the soil. In summary, Fig. 3 shows only the potential vegetation distributions, since it does not include the anthropogenic land use changes.

The expansion of forests and shrinking of grasslands and deserts decreases the albedo (Fig. 4a) and warms the surface (Fig. 4b) via increased absorption of solar radiation. The surface warming, in turn, leads to further forest expansion and changes in the spatial distributions of other vegetation types (Table 2). The local changes in albedo and surface temperature are as large as $-25\%$ and $+8$ K, respectively, in Siberia and Canada. The land-only mean temperature change in the Northern Hemisphere high latitudes (50°N to 90°N) is 2.6 K (Table 3) and the corresponding increase in the net surface absorbed short wave flux is 12.5 $Wm^{-2}$. This warming is in agreement with previous studies (Hansen et al., 1997; Levis et al., 1999; Betts, 2000; Govindasamy et al., 2001; Gibbard et al., 2005), which implied that increased temperate and boreal forest cover lead to warming through a decreased surface albedo, especially at high latitudes (since snow-covered vegetation has much lower albedo than snow-covered bare ground). Local warming of lesser magnitude (2–4 K) is simulated over Europe, Australia, South Africa and eastern parts of North America and South America (Fig. 4b).

The average land-only annual mean warming in the Northern Hemisphere mid-latitudes (20°N to 50°N), Tropics (20°S to 20°N) and Southern Hemisphere mid-latitudes (50°S to 20°S) are 1.5, 0.9 and 1.1 K, respectively (Table 3). As in NH high-latitudes, albedo effects dominate in the NH mid-latitudes with associated increases in net surface solar absorption. In the Tropics and SH mid-latitudes, the albedo decrease is small (Fig. 4a; Table 3), and instead there are increases in the cloudiness, atmospheric column water vapour, and downwelling surface long wave radiation. We caution that the multivariate climate change indicated by Table 3 does not distinguish 'causes' from 'effects' because it includes the results of all the feedbacks. A detailed feedback analysis is beyond the scope of this paper. Because the increased cloudiness has resulted in reduced downwelling solar radiation and solar absorption at the surface, short wave cloud feedbacks are unlikely to be the primary source of the warming.

*Table 3.* Changes in average land-only annual means of climate variables by latitude belt in the Physiol-noGHG case (decade of 2291–2300 minus 1891–1900). The changes are corrected for the drift in the Control simulation. Decrease in the surface albedo appears to be the main source of warming in the NH high and mid-latitudes. In the Tropics and SH mid-latitudes, there are increases in cloudiness, column water vapour, and downwelling long wave radiation, suggesting that cloud/water vapour feedback is the source of the surface warming

| Variable | All land | SH mid –lat 50°S to 20°S | Tropics 20°S to 20°N | NH mid-lat 20°N to 50°N | NH high-lat 50°N to 90°N |
|---|---|---|---|---|---|
| Sfc.Temp. (K) | 1.41 | 1.06 | 0.94 | 1.52 | 2.56 |
| Albedo (%) | −2.3 | −1 | −0.5 | −1.5 | −7.7 |
| LAI ($m^2/m^2$) | 4.06 | 5.88 | 6.91 | 2.87 | 2.10 |
| Sfc. net SW flux ($Wm^{-2}$) | 2.33 | 0.42 | −3.54 | 2.73 | 12.52 |
| Sfc. net LW flux ($Wm^{-2}$) | 2.52 | 2.53 | 0.06 | 2.54 | 7.50 |
| Sensible heat flux ($Wm^{-2}$) | −0.98 | −4.04 | −3.88 | −0.85 | 4.06 |
| Latent heat flux ($Wm^{-2}$) | 0.65 | 2.1 | 0.13 | 0.52 | 1.00 |
| Total cloud (%) | 0.19 | 0.75 | 1.65 | −0.08 | −3.53 |
| Low cloud (%) | −0.97 | 0.80 | 1.77 | −1.14 | −6.24 |
| Sfc. SW down ($Wm^{-2}$) | −0.74 | −2.17 | −5.60 | −0.06 | 6.22 |
| Sfc. LW down ($Wm^{-2}$) | 4.47 | 3.25 | 5.38 | 5.23 | 3.86 |
| Column water vapour (mm) | 0.58 | 0.06 | 0.77 | 0.65 | 0.72 |

We instead infer that the net tropical and SH mid-latitude warming is probably due primarily to cloud/water vapour long wave feedbacks that are initiated by physiological changes to the vegetation.

Because the leaf area index (LAI) and latent heat flux increase in all land areas (Table 3), it is likely that the increases in evapotranspiration (and hence latent heat flux) due to increased leaf area (cooling effect; Betts et al., 1997) dominates over the decrease due to reduced stomatal conductance (warming effect; Sellers et al., 1996). The net surface long wave heat loss also increases in all land areas (Table 3) because of the increase in the LAI and the associated increase in the surface emissivity (Levis et al., 1999). Cooling associated with increases in both the fluxes of latent heat and of the net surface long wave radiation tends to offset part of the warming.

## 5. Discussion

This study demonstrates that the biogeophysical effects of $CO_2$ fertilization could have non-negligible effect on centennial timescales. To some extent, these results may depend on the chosen model and/or experimental set-up. Our terrestrial biosphere model, IBIS2, exhibits higher uptake in comparison to other models (Fig. 2; Prentice et al., 2001), and thus, our estimate of the biogeophysical climate impact of $CO_2$ fertilization is perhaps closer to the upper limit of possible outcomes. The higher sensitivity of IBIS2 to $CO_2$ fertilization may be associated with the lack of nutrient cycles (Thompson et al., 2004). In addition, we have not prescribed realistic future land use change, so as to correctly account for the different effects of crops and natural ecosystems, which might produce overall cooling. For example, Govindasamy et al. (2001) and Brovkin et al. (1999) simulated a global cooling of –0.25 K and –0.35 K, respectively, due to changes from potential natural vegetation to the present-day vegetation distribution. Therefore, our simulated biogeophysical effect of climate warming due to $CO_2$ fertilization could be partially offset by human-induced deforestation, which would produce cooling via increases in the surface albedo. On the other hand, the biogeophysical warming effects could also be enhanced by an anthropogenic land cover change such as afforestation that might be promoted for the purpose of sequestering atmospheric carbon dioxide.

The relative importance of the biogeophysical and the biogeochemical effects of $CO_2$ fertilization can be assessed by estimating the possible climate consequences of $CO_2$ fertilization on atmospheric $CO_2$ concentrations. At the end of our simulations, the land biosphere contains ∼2500 Pg more carbon in the Physiol-noGHG case than in the Control case. If half of this 2500 PgC were to remain in the atmosphere in the absence of $CO_2$ fertilization, then the atmosphere would contain an additional 1250 PgC, or about another 590 ppmv $CO_2$. If this 590 ppmv were added to the 1166 ppmv in the atmosphere at the end of the Physiol-noGHG simulation, it would produce an equilibrium warming of ∼1.2 K, given our model's estimated climate sensitivity of 2.1 K, and a radiative forcing of 3.4 $Wm^{-2}$ per $CO_2$-doubling.

This suggests that for our model and emission scenario, the biogeochemical climate effects of $CO_2$ fertilization would produce 1.2 K global cooling, but the biogeophysical effects would produce a global warming of 0.65 K. These effects are opposite in sign, but are of the same order of magnitude. Moreover, the change in atmospheric $CO_2$ resulting from a land cover change will diminish over time, whereas the dominant biogeophysical effect of reduced albedo will persist; the perturbation to atmospheric $CO_2$ content would be damped by equilibration with the ocean and ultimately with the rock cycles. Therefore, we infer that the biogeophysical climatic effects of land cover

change induced by $CO_2$ fertilization could cancel most of the biogeochemical effects, especially regionally and on centennial timescales. Additional research is needed to better quantify these effects.

## 6. Acknowledgments

This work was performed under the auspices of the U.S. Department of Energy by the University of California Lawrence Livermore National Laboratory under contract No. W-7405-Eng-48. We thank Drs David Lobell, R. Betts and an anonymous reviewer for their helpful comments and suggestions.

## References

Bala, G., Caldeira, K., Mirin, A., Wickett, M. and Delire, C. 2005. Multi-century changes to global climate and carbon cycle: Results from a coupled climate and carbon cycle model. *J. Climate* **18**, 4531–4544.

Betts, R. A. 2000. Offset of the potential carbon sink from boreal forestation by decreases in surface albedo. *Nature* **408**, 187–200.

Betts, R. A., Cox, P. M., Lee, S. E. Woodward, F. I. 1997. Contrasting physiological and structural vegetation feedbacks in climate change simulations. *Nature* **387**, 796–799.

Bonan, G. B., Pollard, D. and Thompson, S. L. 1992. Effects of boreal forest vegetation on global climate. *Nature* **359**, 716–718.

Brovkin, V., Ganapolski, A., Claussen, M., Kubatzki, C. and Petoukhov, V. 1999. Modeling response to historical land cover change. *Global Eco. Biogeo.* **8**, 509–517.

Cox, P. M., Betts, R. A., Jones, C. D., Spall, S. A. and Totterdell, I. J. 2000. Acceleration of global warming due to carbon-cycle feedbacks in a coupled model. *Nature* **408**, 184–187.

Foley, J. A., Kutzbach, J. E., Coe, M. T. and Levis, S. 1994. Feedbacks between climate and boreal forests during the Holocene epoch. *Nature* **371**, 52–54.

Foley, J. A., Prentice, I. C., Ramankutty, N., Levis, S., Pollard, D. and co-authors. 1996. An integrated biosphere model of land surface processes, terrestrial carbon balance and vegetation dynamics. *Global Biogeochem. Cycles* **10**, 603–628.

Friedlingstein, P., Bopp, L., Clais, P., Dufresne, J.-L., Fairhead, L. and co-authors. 2001. Positive feedback between future climate change and the carbon cycle. *Geophys. Res. Lett.* **28**, 1543–1546.

Gedney, N., Cox, P. M., Betts, R. A., Boucher, O. Huntingford, C. and co-authors. 2005. Detection of direct carbon dioxide effect in continental river runoff records. *Nature* **439**, 835–836.

Gibbard, S., Caldeira, K., Bala, G., Phillips, T. J. and Wickett, M. 2005. Climate effects of global land cover change. *Geophys. Res. Lett.* **32**, doi:10.1029/2005GL024550.

Govindasamy, B., Duffy, P. B. and Caldeira, K. 2001. Land use changes and Northern Hemisphere cooling. *Geophys. Res. Lett.* **28**(2), 291–294.

Govindasamy, B., Thompson, S., Caldeira, K., Mirin, A., Wickett, M. and Delire, C. 2005. Increase of carbon cycle feedback with climate sensitivity: results from a coupled climate and carbon cycle model. *Tellus* **57B**, 153–163.

Grace, J., Berninger, F. and Nagy, E. 2002. Impacts of climate change on the tree line. *Ann. Botany* **90**, 537–544.

Henderson-Sellers, A., McGuffie, K., and Gross, C. 1995. Sensitivity of global climate model simulations to increased stomatal resistance and $CO_2$ increases. *J. Climate* **8**, 1738–1756.

Hansen, J., Sato, Mki., Lacis, A. and Ruedy, R. 1997. The missing climate forcing. *Phil. Trans. Royal Soc. London B* **352**, 231–240.

Houghton, R. 2003. Revised estimates of the annual net flux of carbon to the atmosphere from changes in land use and land management 1850-2000. *Tellus* **55B**, 378–390.

Intergovernmental Panel on Climate Change (IPCC) 2001. *Climate Change 2001 The Scientific Basis*. Cambridge University Press, New York.

Kiehl, J. T., Hack, J. J., Bonan, G. B., Boville, B. Y., Briegleb, B. P. and co-authors 1996. Description of the NCAR Community Climate Model (CCM3). *NCAR Tech. Note*. NCAR/TN-420+STR, National Center for Atmospheric Research, Boulder, Colorado.

Kucharik, C. J., Foley, J. A., Delire, C., Fisher, V. A., Coe, M. T. and co-authors. 2000. Testing the performance of a dynamic global ecosystem model: water balance, carbon balance, and vegetation structure. *Global Biogeochem. Cycles* **14**(3), 795–825.

Levis, S., Foley, J. A., and Pollard, D. 1999. Potential high-latitude vegetation feedbacks on CO2-induced climate change. *Geophys. Res. Lett.* **26**(6), 747–750.

Levis, S., Foley, J. A. and Pollard, D. 2000. Large-scale vegetation feedbacks on a doubled $CO_2$ climate. *J. Climate* **13**, 1313–1325.

Lloyd, J. and Taylor, J. A. 1994. On the temperature-dependence of soil respiration. *Funct. Ecol.* **8**, 315–323.

Meehl, G. A., Washington, W. M., Arblaster, J. M. and Hu, A. 2004. Factors affecting climate sensitivity in global coupled models. *J. Climate* **17**, 1584–1596.

Maltrud, M. E., Smith, R. D., Semtner, A. J. and Malone, A. J. 1998. Global eddy-resolving ocean simulations driven by 1985-1995 atmospheric winds. *J. Geophys. Res.* **103**, 30 825–30 853.

Marland G., Boden, T. and Andre, R. 2002. Global, regional, and national annual $CO_2$ emissions from fossil-fuel burning, cement production and gas flaring: 1751-1999, *CDIAC NDP-030*, Carbon Dioxide Information Analysis Center, Oak Ridge National Laboratory, Tennessee.

Mathews, H. D., Weaver, A. J. and Meissner, K. J. 2005. Terrestrial carbon cycle dynamics under recent and future climate change. *J. Climate* **18**, 1609–1628.

Metz, B., Davidson, O., Swart, R. and Pan, J. (eds.) 2001. *Climate Change 2001: Mitigation* (Contribution of Working Group III to the Third Assessment Report of the IPCC), Cambridge Univ. Press, Cambridge.

Najjar, R. G. and Orr, J. C. 1999. Biotic How-To, Revision 1.7, Ocean Carbon-cycle Model Intercomparison Project (OCMIP), http://www.ipsl.jussieu.fr/OCMIP/phase2/simulations/Biotic/HOWTO-Biotic.html.

Notaro, M., Liu, Z., Gallimore, R., Vavrus, S. J., Kutzbach, J. E. and co-authors. 2005. Simulated and observed pre-industrial to model vegetation and climate changes. *J. Climate* **18**, 3650–3671.

Owensby, C. E., Ham, J. M., Knapp, A. K. and Auen, L. M. 1999. Biomass production and species composition change in a tall grass prairie ecosystem after long-term exposure to elevated atmospheric $CO_2$. . *Global Change Biology* **5**, 497–506.

Polley, H. W., Johnson, H. B., Marino, B. D. and Mayeux, H. S. 1993. Increase in C3 plant water-use efficiency and biomass over glacial to present $CO_2$ concentrations. *Nature* **361**, 61–64.

Prentice, I. C., Farquhar, G. D., Fasham, M. J. R., Goulden, M. L., Heimann, M. and co-authors. 2001. *Climate Change 2001: The Scientific Basis: Contribution of Working Group I to the Third Assessment Report of the IPCC* (eds.J. T. Houghton et al.). Cambridge University Press, UK, pp. 183–237.

Ramankutty, N., Foley, J. A., Norman, J. and McSweeney, K. 2002. The global distribution of cultivable lands: current patterns and sensitivity to possible climate change. *Global Ecol. Biogeogr.* **11**, 377–392.

Sellers, P. J., Bounoua, L., Collatz, G. J. and co-authors. 1996. Comparison of radiative and physiological effects of doubled atmospheric $CO_2$ on climate (eds P. J. Sellen et al). *Science* **271**, 1402–1406.

Thompson, S., Govindasamy, B., Mirin, A., Caldeira, K., Delire and co-authors. 2004. Quantifying the effects of CO2-fertilized vegetation on future global climate and carbon dynamics. *Geophys. Res. Lett.* **31**(23), L23211.

Zeng, N., Qian, H., Munoz, E. and Iacono, R. 2004. How strong is carbon cycle-climate feedback under global warming? *Geophys. Res. Lett.* **31**, doi:10.1029/ 2004GL020904.